Journal of Circuits, Systems, and Computers, Vol. 3, No. 1 (1993) 33–48

BISPECTRAL ANALYSIS OF CHUA'S CIRCUIT

STEVE ELGAR

School of Electrical Engineering and Computer Science, Washington State University, Pullman, WA 99164-2752, USA

and

MICHAEL PETER KENNEDY

Department of Electronic and Electrical Engineering, University College Dublin, Dublin 4, Ireland

Received 10 April 1992
Revised 11 June 1992

Bispectral analysis (which isolates quadratic nonlinear interactions among triads of Fourier components) is used to investigate bifurcations in Chua's circuit. For period-doubled limit cycles, the dominant interactions of the circuit are quadratically nonlinear, and bicoherence spectra isolate the phase coupling between increasing numbers of triads of Fourier components as the nonlinearity of the system is increased. For circuit parameters that result in a chaotic, Rössler-type attractor, bicoherence spectra indicate that quadratic nonlinear interactions are important to the dynamics. For parameters that lead to the double scroll chaotic attractor the bispectrum is zero, suggesting that nonlinear interactions of order higher than quadratic dominate the dynamics. Higher-than-second order spectra (e.g. trispectra) are required to isolate the individual nonlinear interactions for the double scroll.

1. Introduction

Since their introduction almost thirty years ago,[1] bispectral and other polyspectral techniques have been used to study many nonlinear systems, including fluid[2–10] mechanical,[11–14] and quantum-mechanical systems.[15,16] Bispectral analysis isolates the nonlinearly-induced phase coupling between triads of Fourier modes in quadratically nonlinear systems. This phase coupling can lead to cross-spectral transfers of energy (e.g. growth of super and/or subharmonics) and to non-Gaussian statistics (e.g. nonsinusoidal wave profiles).

Another quantitative measure of nonlinear systems is the fractal dimension, including the Grassberger-Procaccia, or correlation dimension,[17–19] the averaged pointwise dimension,[20] and the Lyapunov dimension.[21] Along with dimension, numerically generated or experimentally observed time series can be characterized by power spectra, phase space portraits, Poincaré sections, and Lyapunov exponents[22–24] and many others. Although these methods of modern nonlinear dynamics have been extremely valuable for investigating nonlinear systems, they do not present information about nonlinear interactions between the Fourier components of the system.

The primary purpose of the present study is to combine bispectral analysis with nonlinear dynamics analysis to obtain further understanding of the underlying physics of Chua's circuit (Chua, 1992).[25] In particular, a single state variable is analyzed as the system follows a period-doubling route to chaos to determine which modes of motion are interacting with each other. The chaotic state which results from this period-doubling cascade corresponds to a Rössler-like attractor. Although the Rössler equations are quadratically nonlinear (Thompson and Stewart[26] and references therein), while Chua's equation is piecewise-linear, bispectral analysis suggests that quadratic nonlinear modal interactions are important in both cases.

In contrast, the double scroll chaotic attractor which appears in Chua's circuit[27] is *not* dominated by quadratic nonlinearities, as demonstrated by low bicoherence values. Higher-than-second-order spectral analysis is necessary to investigate the modal interactions for the double scroll.

Definitions and properties of the bispectrum are reviewed in Sec. 2. Phase planes, power spectra, and bicoherence spectra for experimental data obtained from Chua's circuit are discussed in Sec. 3, followed by conclusions in Sec. 4.

2. Definitions and Properties of the Bispectrum

Let a stationary random process be represented as

$$\eta(t) = \sum_{n=1}^{N} A_n e^{i\omega_n t} + A_n^* e^{-i\omega_n t} \tag{1}$$

where ω is the radian frequency, the subscript n is a frequency (modal) index, asterisk indicates complex conjugation, and the A_n are complex Fourier coefficients. The auto-bispectrum is formally defined as the Fourier transform of the third-order correlation function of the time series[1]

$$B(\omega_1, \omega_2) = \left(\frac{1}{2\pi}\right)^2 \int_{-\infty}^{\infty} \int_{-\infty}^{\infty} S(\tau_1, \tau_2) e^{-i\omega_1\tau_1 - i\omega_2\tau_2} d\tau_1 d\tau_2 \tag{2}$$

where

$$S(\tau_1, \tau_2) = E[\eta(t)\eta(t+\tau_1)\eta(t+\tau_2)] \tag{3}$$

with $E[\cdot]$ the expected-value, or average, operator. The discrete bispectrum, appropriate for discretely sampled data, is[28,29]

$$B(\omega_k, \omega_j) = E[A_{\omega_k} A_{\omega_j} A^*_{\omega_k+\omega_j}] \,. \tag{4}$$

Similarly, the power spectrum is defined here as

$$P(\omega_k) = \frac{1}{2} E[A_{\omega_k} A^*_{\omega_k}]. \tag{5}$$

From (4) the bispectrum is zero if the average triple product of Fourier coefficients is zero. This occurs if the modes are independent of each other, i.e. for the random phase relationships between Fourier modes in a linear process. Using symmetry properties, the bispectrum can be uniquely described by its values in a bifrequency octant. For a discrete time series with Nyquist frequency ω_N, the bispectrum is uniquely defined within a triangle in (ω_1, ω_2)-space with vertices at $(\omega_1 = 0, \omega_2 = 0), (\omega_1 = \omega_{N/2}, \omega_2 = \omega_{N/2})$, and $(\omega_1 = \omega_N, \omega_2 = 0)$.

It is convenient to recast the bispectrum into its normalized magnitude and phase, called the bicoherence and biphase, given respectively by[29]

$$b^2(\omega_1, \omega_2) = \frac{|B(\omega_1, \omega_2)|^2}{E[|A_{\omega_1} A_{\omega_2}|^2] E[|A_{\omega_1+\omega_2}|^2]} \tag{6}$$

$$\beta(\omega_1, \omega_2) = \arctan\left[\frac{-\mathrm{Im}\,\{B(\omega_1, \omega_2)\}}{\mathrm{Re}\{B(\omega_1, \omega_2)\}}\right]. \tag{7}$$

For a three-wave system, Kim and Powers show that $b^2(\omega_i, \omega_j)$ represents the fraction of power at frequency $\omega_i + \omega_j$ owing to quadratic coupling of the three modes $(\omega_i, \omega_j$, and $\omega_i + \omega_j)$. No such simple interpretation for the bicoherence is possible in a broadband process where a particular mode may be simultaneously involved in many interactions.[30] Nevertheless, the bicoherence does give an indication of the relative degree of phase coupling between triads of Fourier components, with $b = 0$ for random phase relationships, and $b = 1$ for maximum coupling.

The biphase is related to the shape (in a statistical sense) of the time series.[31,32]

For a finite length time series even a truly Gaussian process will have a nonzero bispectrum. A 95% significance level on zero bicoherence is given by Haubrich[28] as

$$b^2_{95\%} = 6/\mathrm{d.o.f.} \tag{8}$$

where d.o.f. is the number of degrees of freedom. All bicoherences presented below are significant at the 95% level. Tests with different windows and record lengths indicate that the power spectra and bispectra presented here are not significantly affected by leakage or smearing.

3. Chua's Circuit

In this section phase plane portraits, power spectra, and bicoherence spectra for data measured from Chua's circuit are presented.

Chua's circuit (Fig. 1) consists of an inductor L, two capacitors C_1 and C_2, a linear resistor R, and a nonlinear resistor N_R. This circuit is described by a set of three ordinary differential equations[27,33]

$$\begin{aligned} C_1 \frac{dv_{C_1}}{dt} &= G(v_{C_2} - v_{C_1}) - g(v_{C_1}) \\ C_2 \frac{dv_{C_2}}{dt} &= G(v_{C_1} - v_{C_2}) + i_L \end{aligned} \tag{9}$$

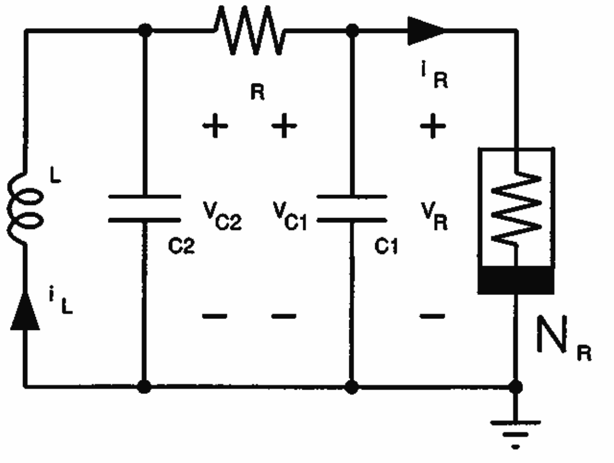

Fig. 1. Chua's circuit, consisting of a linear inductor, L, a linear resistor, R, two linear capacitors, C_1, C_2, and a nonlinear resistor, N_R.

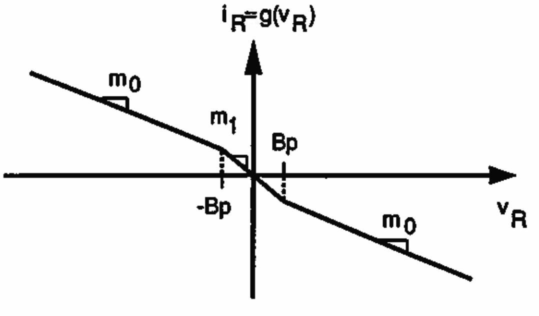

(a)

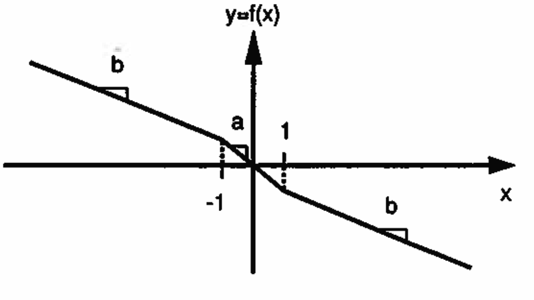

(b)

Fig. 2. (a) Three segment, piecewise-linear v–i characteristic of the nonlinear resistor in Chua's circuit. The outer regions have slopes m_0 and the inner region has slope m_1. The breakpoints in slope are denoted by $-B_p, B_p$ (b) in dimensionless form, the breakpoints are at ± 1. The inner and outer regions of the characteristic have slopes a and b respectively.

$$L\frac{di_L}{dt} = -v_{C_2}$$

where v_{C_1} and v_{C_2} are the voltages across capacitors C_1 and C_2 respectively, and i_L is the current flowing upwards through the inductor. G denotes the conductance of R ($G = 1/R$) and $g(\cdot)$ is a piecewise-linear function (Fig. 2) given by

$$g(v_R) = m_0 v_R + 0.5(m_1 - m_0)(|v_R + B_p| - |v_R - B_p|). \tag{10}$$

Chua's circuit has been studied extensively both experimentally and analytically and has been shown to exhibit every type of bifurcation and attractor reported for a third-order continuous time dynamical system (for a comprehensive bibliography of papers on Chua's circuit see Ref. 34).

Most analytical studies of Chua's circuit have investigated a dimensionless form of the equations obtained by rescaling the parameters of the system.

Defining

$$x = v_{C_1}/B_p; y = v_{C_2}/B_p; z = i_L/(B_p G)$$
$$\tau = tG/C_2; a = m_1/G; b = m_0/G$$
$$\alpha = C_2/C_1; \beta = C_2/(LG^2)$$

the dimensionless equations become

$$\begin{aligned} \frac{dx}{d\tau} &= \alpha(y - x - f(x)) \\ \frac{dy}{d\tau} &= x - y + z \\ \frac{dz}{d\tau} &= -\beta y \end{aligned} \tag{11}$$

where (see Fig. 2(b))

$$f(x) = bx + \frac{1}{2}(a - b)\left[|x+1| - |x-1|\right] \tag{12}$$

Realizations of Chua's circuit can be obtained using standard or custom-made components. While the linear elements are readily available as two-terminal devices, the nonlinear resistor (a Chua diode[34]) must be constructed from active circuit elements. Figure 3 shows the implementation of Chua's circuit[35] used in the present study. Here, N_R consists of a negative impedance converter N_{R_1} and two ideal-diode[36] subcircuits N_{R_2} and N_{R_3} which determine the breakpoints B_p and $-B_p$ in the v–i characteristic (Figure 2). A complete list of the circuit elements is given in Table 1. By fixing all components and varying only the capacitance C_1, the parameter α in the normalized equations (11) can be adjusted.

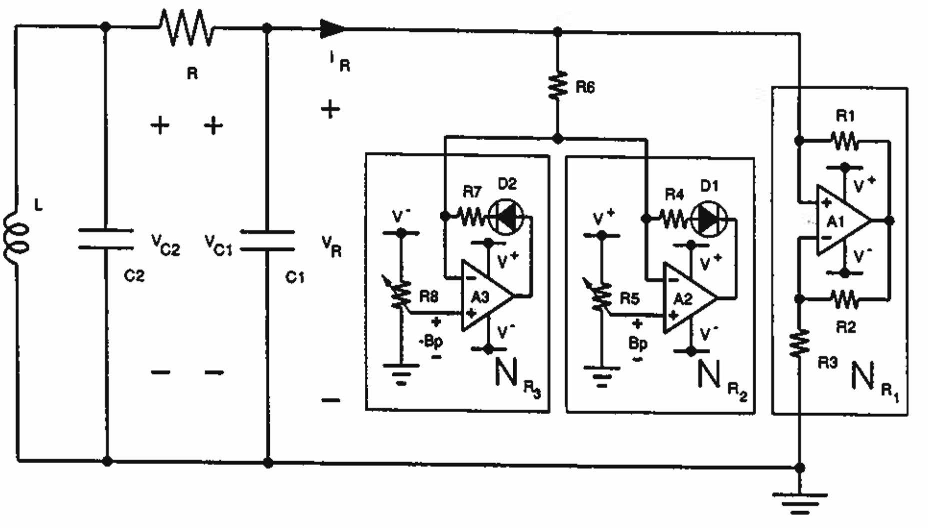

Fig. 3. Experimental realization of Chua's circuit used in this study.

Table 1. Components and circuit parameters common to all time series. The corresponding normalized circuit parameters are $a = -R/R_3 = -1.14$, $b = R/R_3 + R/R_6 = -0.712$, and $\beta = R^2C_2/L = 14.38$.

Parameter	Value
L	12.44 mH
C_2	178.5 nF
R	1.001 kΩ
R_1	150.0 Ω
A_1	AD711KN op amp
R_2	150.0 Ω
R_3	878.1 Ω
R_4	2.2 kΩ
D_1	1N4148 silicon switching diode
A_2	$\frac{1}{2}$AD712KN dual op amp
R_5	10 kΩ
B_p	1 V
R_6	2.339 Ω
R_7	2.2 kΩ
D_2	1N4148 silicon switching diode
A_3	$\frac{1}{2}$AD712KN dual op amp
R_8	10 kΩ
$-B_p$	−1 V

3.1. *Experimental results for Chua's circuit*

A period-doubling sequence and two chaotic states, corresponding to a Rössler attractor (a model of the Lorenz attractor, Thompson and Stewart[25] and references therein) and to the double scroll[27] were examined.

Five time series of the voltage wave form v_{C_1} (equivalently, the dimensionless variable x) for five different values of the capacitance C_1 (Table 2) were recorded. Analog-to-digital conversion was achieved by means of a 16-bit data acquisition board with fourth-order lowpass (20 kHz corner frequency) filters. The data acquisition board was preceded by an amplifier whose gain was adjusted to match the signal level to the input dynamic range of the convertor. The sampling frequency was 49.9 kHz.

Table 2. Values of C_1 and $\alpha = C_2/C_1$ for the five case studies discussed in the text.

Case	C_1	α
Period 1	17.5 nF	10.20
Period 2	17.2 nF	10.38
Period 4	16.9 nF	10.56
Rössler	16.6 nF	10.75
Double scroll	15.0 nF	11.92

Power and bicoherence spectra were calculated by subdividing the voltage time series into 192 short records, each 512 points long. A Hanning window with 75% overlap was applied to each short time series to reduce spectral leakage, and power spectra and bispectra from each of the 192 records were ensemble, averaged producing estimates with 384 degrees of freedom and a final frequency resolution of 0.097 kHz.

Ordinary power spectral analysis cannot detect the phase coupling between Fourier components, nor the cross-spectral transfer of energy between motions at the primary spectral peak frequency and motions at sub- and super-harmonics, because the power spectrum does not contain any phase information. On the other hand, Chua's circuit undergoes a period-doubling route to chaos, which is usually associated with quadratic nonlinear interactions, and thus bispectral analysis may be used to investigate the coupling of/and energy exchange between the various components of the system.

Phase plane portraits for period-1, period-2, and period-4 limit cycles of Chua's circuit are shown in Fig. 4. Corresponding power spectra are shown in Fig. 5 and are characterized by narrow spectral peaks. The harmonic structure of the attractor is clearly displayed in the power spectra (Fig. 5). For period-1 motion, the spectrum is dominated by a primary spectral peak with frequency $f = 2.5$ kHz, and its higher

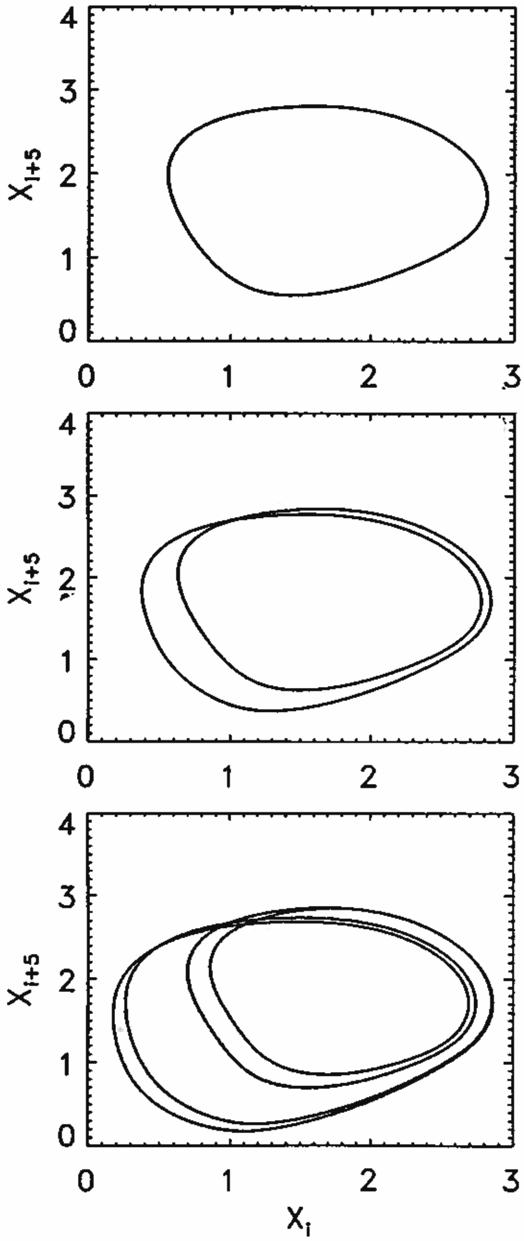

Fig. 4. Reconstructed phase portraits for voltage v_{C_1} measured from Chua's circuit. The voltage at time $i + 5$ is plotted versus the voltage at time i. The delay of five samples corresponds to approximately 1/4 cycle of the power spectral primary peak frequency. Top to bottom, period-1 limit cycle, period-2 limit cycle, period-4 limit cycle. The corresponding circuit parameters are given in Tables 1 and 2.

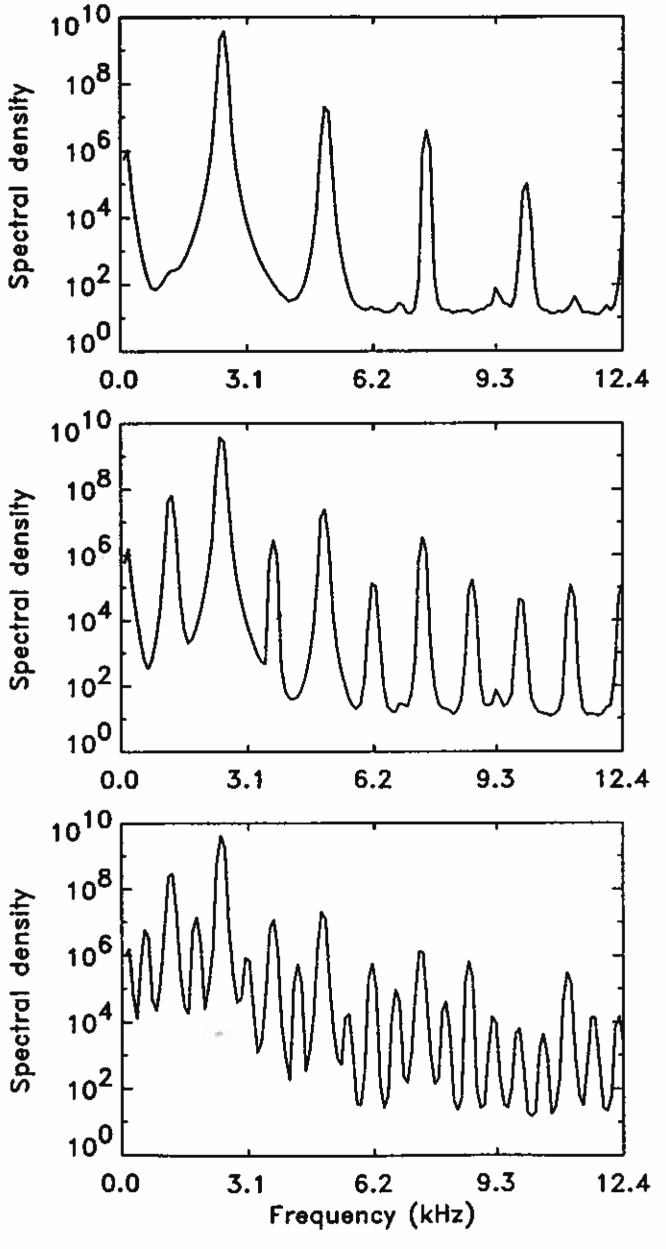

Fig. 5. Power spectra of voltages measured from Chua's circuit. Top to bottom, period-1 limit cycle, period-2 limit cycle, period-4 limit cycle. The corresponding circuit parameters are given in Tables 1 and 2. The units of power are arbitrary.

harmonics. As α is increased, the subharmonic ($f = 1.25$ kHz) is excited (period-2 motion) and, owing to quadratic nonlinearities, the spectrum contains peaks at frequencies corresponding to sum interactions of the subharmonic, the primary, and their harmonics. As α is increased further, another period-doubling occurs ($f = 0.625$ kHz is excited, period-4 motion), and the power spectrum (Fig. 5) contains many peaks, corresponding to the two subharmonics, the primary, and their combination tones.

The quadratic interactions between triads of Fourier modes for Chua's circuit are isolated by the bicoherence spectrum as shown in Fig. 6. For the period-1 case, bicoherence spectra clearly show the coupling between motions at the primary spectral peak frequency and its harmonics, as well as between the first and second harmonics, the first and third harmonics, and so on. The high bicoherence values associated with $f_2 = 2.5$ kHz indicate nonlinear energy transfer from the primary to the higher-frequency modes. The interactions are restricted to triads of Fourier components that include the primary and its harmonics.

Power spectra for the period-2 case (Fig. 5) show narrow peaks between the harmonics of the primary peak. The corresponding bicoherence spectrum (Fig. 6) shows the coupling between motions at the primary peak frequency ($f = 2.5$ kHz), its harmonics, the period-doubled frequency (subharmonic, $f = 1.25$ kHz), and its harmonics. Quadratic interactions between oscillations at the primary and the period-doubled subharmonic are transferring energy into the higher harmonics, giving a greater number of peaks in the frequency spectrum with a much richer structure than the period-1 case.

For period-4 motion both the power (Fig. 5) and bicoherence (Fig. 6) spectra contain peaks associated with the primary ($f = 2.5$ kHz), both subharmonics ($f = 1.25$ and $f = 0.625$ kHz), and all their combination tones. The bicoherence spectrum indicates that these interactions are quadratic and it delineates precisely which Fourier components are interacting quadratically with each other.

Time series corresponding to the Rössler attractor exhibit similarities to and differences from the period-doubling sequences shown in Figs. 4–6. The Rössler-like attractor is chaotic. Note how the corresponding phase portrait (Fig. 7) differs significantly from those of the relatively simple orbits of the period-doubling sequence (Fig. 4). The Rössler attractor has a fairly broad power spectrum (Fig. 7), with only remnants of the primary and harmonic peaks of the period-doubled cases (Fig. 5). However, as can be seen in the bicoherence spectrum (Fig. 7) quadratic interactions are still important. Motions corresponding to the remnant of the primary peak ($f_2 = 2.5$ kHz) are quadratically coupled to both higher frequencies (horizontal band of contours at $f_2 = 2.5$ kHz) and to lower frequencies (vertical band of contours at $f_1 = 2.5$ kHz). Similar quadratic interactions occur between motions at the harmonics ($f = 5.0$ and $f = 7.5$ kHz) of the primary spectral peak and both higher- and lower-frequency motions. The minimum contour levels shown in the bicoherence spectrum for the Rössler attractor (Fig. 7) is $b = 0.7$. However, bicoherences are statistically significant for many more frequency triads ($b_{95\%} = 0.13$, not shown), indicating that quadratic nonlinear interactions occur between nearly all the frequency components of the Rössler system.

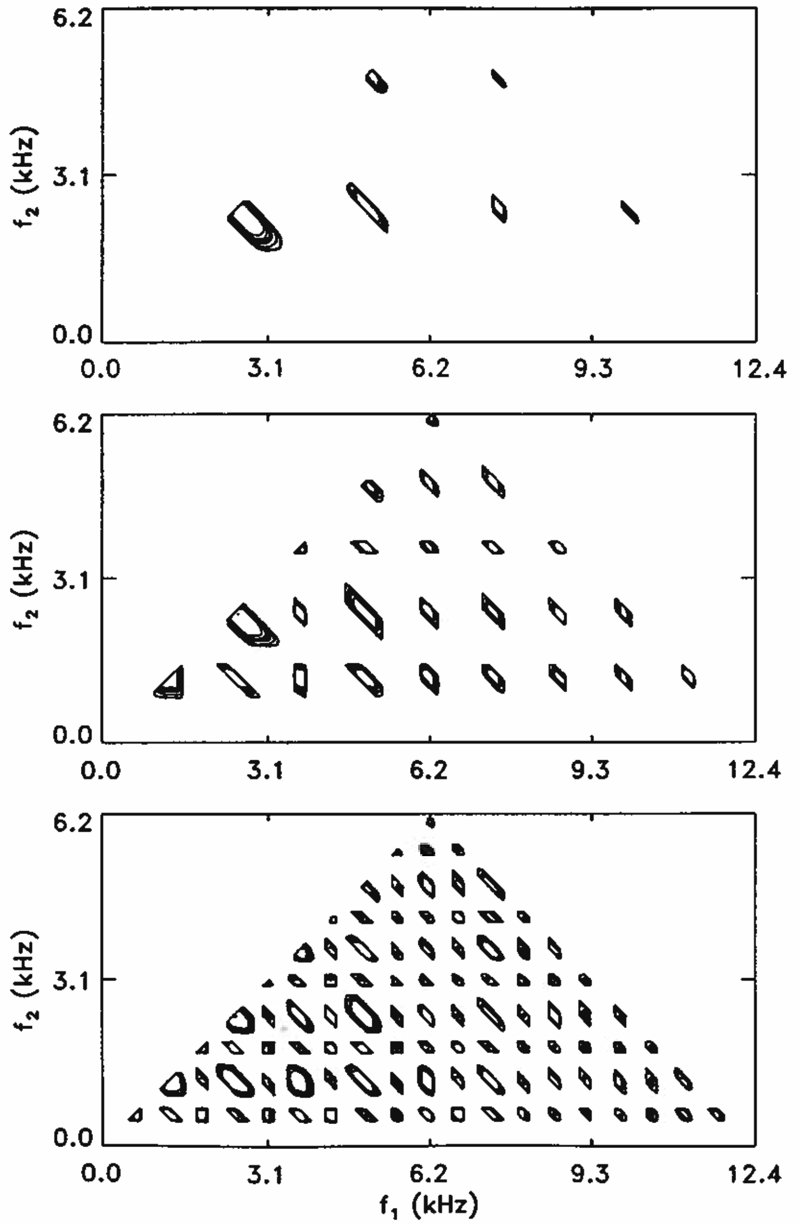

Fig. 6. Bicoherence spectra of voltages measured from Chua's circuit. Contours indicate quadratic phase coupling between motions with frequencies $f_1, f_2, f_1 + f_2$. The minimum contour plotted is $b = 0.98$. Top to bottom, period-1 limit cycle, period-2 limit cycle, period-4 limit cycle. The corresponding circuit parameters are given in Tables 1 and 2.

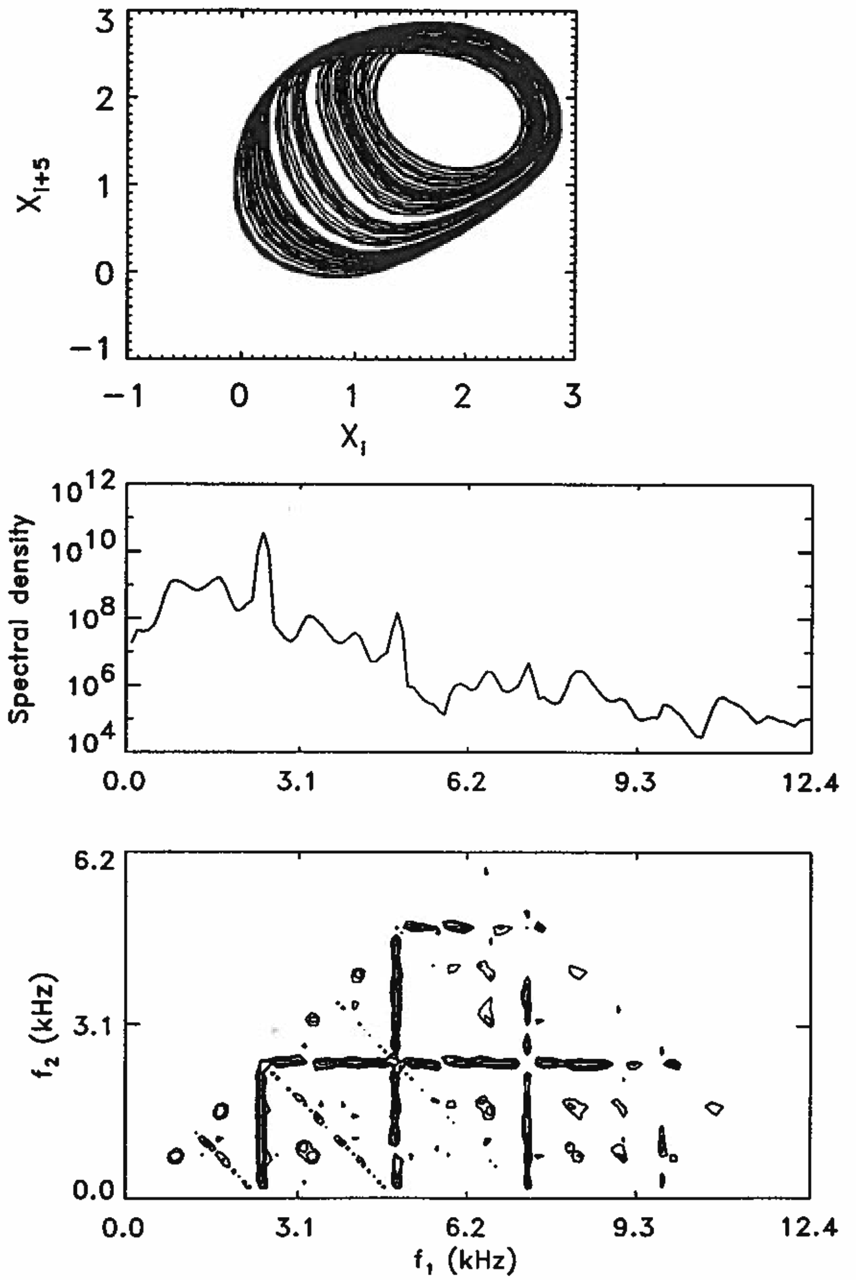

Fig. 7. Reconstructed phase portrait (upper), power spectrum (center), and bicoherence spectrum (lower) for voltage v_{C_1} measured from Chua's circuit when the system exhibits a Rössler-like attractor. The units of power are arbitrary and the minimum contour plotted is $b = 0.7$.

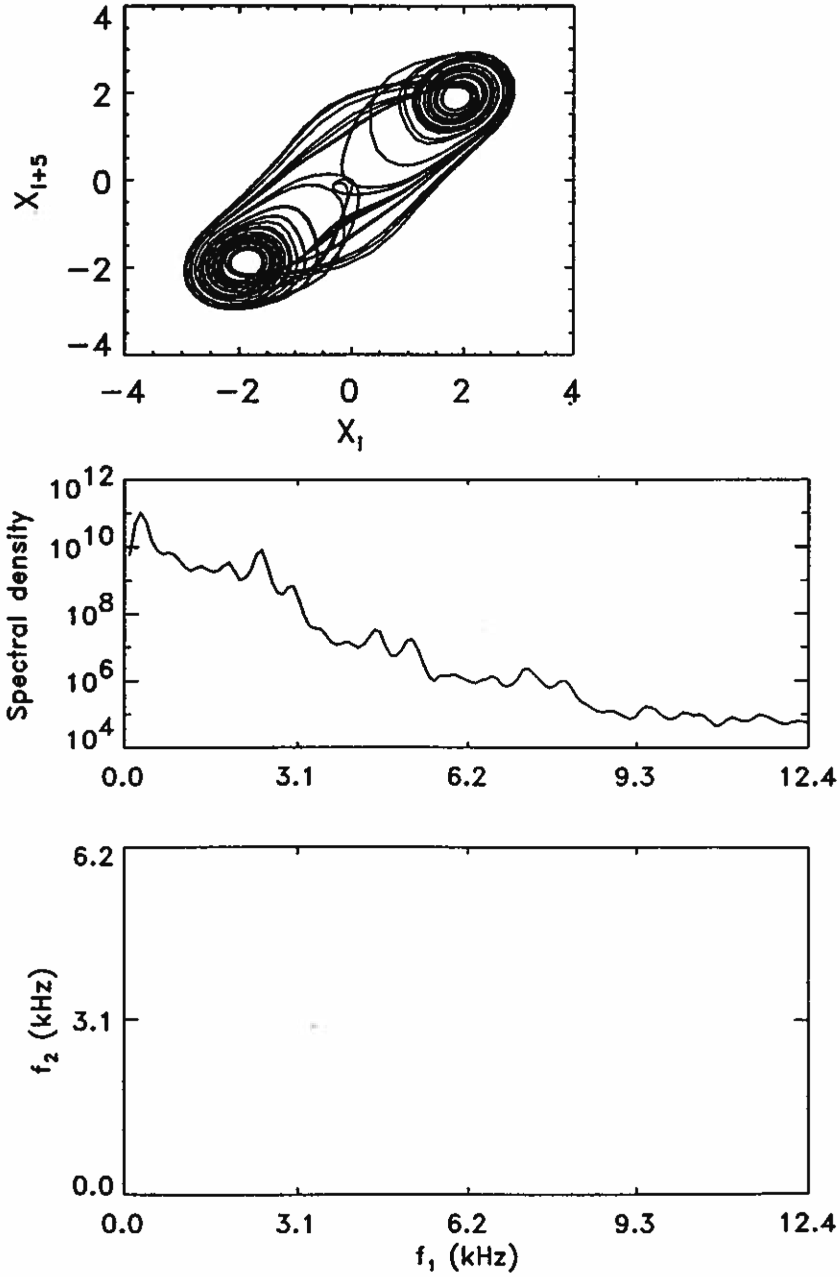

Fig. 8. Reconstructed phase portrait (upper), power spectrum (center), and bicoherence spectrum (lower) for voltage v_{C_1} measured from a double scroll attractor in Chua's circuit. The units of power are arbitrary and there are no contours above $b = 0.13$, the 95% significance level.

Unlike the period-doubled and Rössler attractors, the double scroll (Fig. 8) is not dominated by quadratic interactions. The double scroll attractor can be seen in the phase portrait (Fig. 8). It is characterized by a very broad power spectrum (Fig. 8), with only a vestige of the primary peak (f = 2.5 kHz) and much more energetic low-frequency motions (compare Fig. 8 to Figs. 7 and 5). There are no statistically significant bicoherences (Fig. 8), indicating that the nonlinearities for the double scroll are not quadratic. A Rössler-type attractor in Chua's circuit is confined to two regions of the piecewise-linearity. In contrast, trajectories in the double scroll visit all three regions. While a two-segment nonlinearity can be approximated by a quadratic, the three-segment nonlinearity requires a higher-order approximation. Since the motion is global in nature, the absolute value term dominates the motion, thus leaving only an insignificant amount of quadratic phase coupling and energy transfer in the system's motion. Similar behavior has been observed in the driven Sine-Gordon chain[15] and the Duffing equation.[14] Higher-than-second order spectra are required to isolate the individual interacting Fourier components for the double scroll.

4. Conclusions

As Chua's circuit undergoes a period-doubling sequence to chaos, quadratic nonlinear interactions couple, and transfer energy between, triads of Fourier components. The individual quadratic interactions are isolated by the bicoherence, and bicoherence spectra show increasing numbers of phase coupled components as the nonlinearity of the system is increased. For a period-1 limit cycle, motions at the frequency corresponding to the power spectral peak frequency and its harmonics are coupled. For a period-2 limit cycle, motions at the subharmonic, the primary, and their super harmonic frequencies are quadratically coupled, while for period-4 motion the many combinations of lowest subharmonic, subharmonic, primary, and corresponding super harmonics are quadratically coupled.

When the system becomes chaotic the power spectrum broadens, but in the case of the Rössler attractor, quadratic nonlinear interactions remain important. Motions at the primary frequency and its harmonics are quadratically coupled to motions at many other frequencies. In the case of the double scroll attractor, however, the system is no longer dominated by quadratic nonlinear interactions, and bicoherence values are essentially zero. Higher-order spectra (e.g. trispectra, work in progress) are necessary to isolate the individual nonlinear interactions between Fourier components for the double scroll.

Acknowledgements

We thank Dr. Leon Chua for introducing us to each other and for suggesting the application of bispectral analysis to Chua's equation. Steve Elgar's research is supported by the Office of Naval Research (Coastal Sciences and NOW ARI) and the National Science Foundation (Physical Oceanography). We are grateful to Chai

Wah Wu of U.C. Berkeley for his assistance in acquiring the experimental data for this paper. Michael Peter Kennedy's visiting appointment as Postdoctoral Research Engineer at the Electronics Research Laboratory was funded by the National Science Foundation.

References

1. K. Hasselmann, W. Munk, and G. MacDonald, "Bispectra of ocean waves", *Time Series Analysis*, ed. M. Rosenblatt, John Wiley, New York, pp. 125–139.
2. T. T. Yeh and C. W. Van Atta, "Spectral transfer of scalar and velocity fields in heated-grid turbulence", *J. Fluid Mechanics* **58** (1973) 233–261.
3. K. S. Lii, M. Rosenblatt, and C. Van Atta, "Bispectral measurements in turbulence", *J. Fluid Mechanics* **77** (1976) 45–62.
4. K. N. Helland, C. W. Van Atta, and G. N. Stegun, "Spectral energy transfer in high Reynolds number turbulence", *J. Fluid Mechanics* **79** (1977) 337–359.
5. C. W. Van Atta, "Inertial range bispectra in turbulence", *Physics of Fluids* **22** (1979) 1440–1443.
6. Y. C. Kim, J. M. Beall, E. J. Powers, and R. W. Miksad, "Bispectrum and nonlinear wave coupling", *Phys. Fluids* **21** (1980) 258–263.
7. R. Miksad, F. Jones, and E. Powers, "Measurements of nonlinear interactions during natural transition of a symmetric wake", *Phys. Fluids* **26** (1983) 1402–1408.
8. S. Elgar and R. Guza, "Observations of bispectra of shoaling surface gravity waves", *J. Fluid Mechanics* **161** (1985) 425–448.
9. C. Ritz, E. Powers, R. Miksad, and R. Solis, "Nonlinear spectral dynamics of a transitioning flow", *Phys. Fluids* **31** (1988) 3577–3588.
10. M. Hajj, R. Miksad, and E. Powers, "Subharmonic growth by parametric resonance", *J. Fluid Mechanics* **236** (1992) 385-413.
11. D. Choi, J. H. Chang, R. Stearman, and E. Powers, "Bispectral identification of nonlinear mode interactions", *Proc. 2nd Int. Modal Analysis Conf.*, Vol. II, 1984, pp. 3–12.
12. T. Sato, K. Sasaki, and Y. Nakamura, "Real-time bispectral analysis of gear noise and its application to contactless diagnosis", *J. Acoustical Soc. America* **62** (1977) 382–387.
13. C. Pezeshki, S. Elgar, and R. C. Krishna, "Bispectral analysis of systems possessing chaotic motion", *J. Sound Vibration* **137** (1990) 357–368.
14. C. Pezeshki, S. Elgar, R. C. Krishna, and T. D. Burton, "Auto- and cross-bispectral analysis of a system of two coupled oscillators with quadratic nonlinearities possessing chaotic motion", *J. Applied Mechanics* **59** (1991) 657–663.
15. M. D. Miller, "Bispectral analysis of the driven Sine-Gordon chain", *Phys. Rev.* **B34** (1986) 6326–6333.
16. C. L. Nikias and M. R. Raghuveer, "Bispectrum estimation: A digital signal processing framework", *Proc. IEEE* **75** (1987), 869–891.
17. P. Grassberger and I. Procaccia, "Characterization of strange attractors", *Phys. Rev. Lett.* **50** (1983) 346–349.
18. P. Grassberger and I. Procaccia, "Measuring the strangeness of strange attractors", *Physics* **9D** (1983) 189–208.
19. J. O. Roux, R. H. Simoyi, and H. L. Swinney, "Observation of a strange attractor", *Physica* **8D** (1983) 257–266.
20. J. Farmer, E. Ott, and J. Yorke, "The dimension of chaotic attractors", *Physica* **7D** (1983) 153–179.

21. P. Frederickson, J. Kaplan, E. Yorke, and J. Yorke, "The Lyapunov dimension of strange attractors", *J. Differential Equations* **49** (1983) 185–207.
22. N. H. Packard, J. P. Crutchfield, J. D. Farmer, and R. S. Shaw, "Geometry from a time series", *Phys. Rev. Lett.* **45** (1980) 712–715.
23. A. Wolf, J. B. Swift, H. L. Swinney, and J. A. Vastano, "Determining Lyapunov exponents from a time series", *Physica* **16D** (1985) 285–317.
24. A. Brandstater and H. L. Swinney, "Strange attractors in weakly turbulent Couette–Taylor flow", *Phys. Rev.* **A35** (1987) 2207–2220 and references therein.
25. L. O. Chua, "The genesis of Chua's circuit", *Archiv für Elektronik und Ubertragungstechnik* **46** (1992) 250–257.
26. J. B. Thompson and H. B. Stewart, *Nonlinear Dynamics and Chaos*, John Wiley, New York, 1986, pp. 235–238.
27. L. Chua, M. Komuro, and T. Matsumoto, "The double scroll family", *IEEE Circuits Systems* **33** (1985) 1073–1118.
28. R. A. Haubrich, "Earth noises, 5 to 500 millicycles per second", *J. Geophys. Res.* **70** (1965) 1415–1427.
29. Y. C. Kim and E. J. Powers, "Digital bispectral analysis and its applications to nonlinear wave interaction", *IEEE Trans. Plasma Science* **PS-7** (1979) 120–131.
30. C. McComas and M. Briscoe, "Bispectra of internal waves", *J. Fluid Mechanics* **97** (1980) 205–213.
31. A. Masuda and Y. Kuo, "A note on the imaginary part of the bispectrum", *Deep Sea Research* **28** (1981) 213–222.
32. S. Elgar, "Relationships involving third moments and bispectra of a harmonic process", *IEEE Acoustics, Speech Signal Process.* **35** (1987) 1725–1726.
33. G. Zhong and F. Ayrom, "Experimental confirmation of chaos in Chua's circuit", *Int. J. Circuit Theory Appl.* **13** (1985) 93–98.
34. M. P. Kennedy, "Robust op amp realization of Chua's circuit", *Frequenz* **46** (1992) 66–88.
35. M. P. Kennedy, "Experimental chaos via Chua's circuit", *Proc. of the 1st Experimental Chaos Conf.*, eds. S. Vohra, M. Spano, M. Shlesinger, L. Pecora, and W. Ditto, 1992, pp. 340–351.
36. L. Chua, C. A. Desoer, and E. S. Kuh, *Linear and Nonlinear Circuits*, McGraw-Hill New York, 1987.